Rare Metal Materials and Engineering
Volume 53, Issue 12, December 2024
Available online at www.rmme.ac.cn

Science Press

Cite this article as: Ji Jinjin, Jia Zhi, Yang Peiyao, et al. Effect of Grain Refinement on Microtexture and Mechanical Properties of Inconel 617 Alloy[J]. Rare Metal Materials and Engineering, 2024, 53(12): 3313-3320. DOI: 10.12442/j.issn.1002-185X.20240091.

ARTICLE

Effect of Grain Refinement on Microtexture and Mechanical Properties of Inconel 617 Alloy

Ji Jinjin[1,2,3], Jia Zhi[1,2], Yang Peiyao[1,2], Wang Yanjiang[1,2], Kou Shengzhong[1,2]

[1] School of Materials Science and Engineering, Lanzhou University of Technology, Lanzhou 730050, China; [2] State Key Laboratory of Advanced Processing and Recycling of Nonferrous Metals, Lanzhou University of Technology, Lanzhou 730050, China; [3] School of Materials Engineering, Lanzhou Institute of Technology, Lanzhou 730050, China

Abstract: The microstructure and mechanical properties of Inconel 617 alloy rolled at room temperature with different deformation degrees (20%, 50%, 70%) were investigated. The grain refinement mechanism and main texture types of Inconel 617 alloy during rolling were analyzed via electron backscatter diffraction and X-ray diffraction, and the microhardness and tensile properties of Inconel 617 alloy with different deformation degrees were tested. Results reveal that the grains of Inconel 617 alloy are refined during the rolling deformation process, and the refinement mechanism is the fragmentation of original grains caused by the increase in dislocation density and strain gradient. The main microtextures of the rolled samples are Goss {011}<001>, Rotated Goss {110}<110>, Brass {011}<211>, and P {011}<112> textures, and their intensity is increased with increase in deformation degree. After rolling deformation, the strength of the Inconel 617 alloy is improved and the ductility is reduced by the combined effect of grain refinement and dislocation strengthening. Comprehensively, the yield strength and elongation of Inconel 617 alloy after 20% deformation are 772.48 MPa and 0.1962, respectively, presenting good synergy effect.

Key words: Inconel 617 alloy; grain refinement; microtexture; microhardness; tensile properties

Inconel 617 nickel-based superalloy is widely used in aerospace, marine, and other fields because of its excellent high-temperature microstructure stability and corrosion resistance[1–6]. With the development of industrial technology, the workpiece of Inconel 617 alloy is prone to failure under high temperature environments and extreme stress conditions, which greatly reduces the service life and safety reliability. Accordingly, better performance of Inconel 617 alloy is required. Grain refinement is a common strengthening mechanism in nickel-based superalloys, because the small grain size and high grain boundary fraction can improve the mechanical properties and corrosion resistance of the materials[7–10]. However, with the grain refinement, the material properties, such as microtexture, hardness, and tensile properties, are also changed.

The rolling plastic deformation technique has the advantages of simple operation, wide application field, and remarkably grain refinement effect[11–12]. The rolling process is often used in the forming procedure of nickel-based superalloy workpieces. During the rolling process, the equiaxed grains are transformed into lamellar grains along the rolling direction[13]. With the microstructure evolution, the mechanical properties of materials also change. For example, the dislocation density of Inconel 625 alloy increases significantly after rolling deformation, which results in an increase in yield strength and a decrease in ductility[14]. Polkowska et al[15] studied the effect of cold rolling deformation degrees on the microstructure, recrystallization microtexture, and mechanical properties of Haynes 282 wrought nickel-based superalloy. Liu et al[16] studied the effect of rolling and annealing on the microstructure and mechanical properties and found that the precipitation of carbides and the migration of grain boundaries at high temperatures were the main reasons for cracking. Twinning is the main grain refinement mechanism during rolling and annealing of Inconel 617 alloy[17]. In addition, the

Received date: February 25, 2024
Foundation item: Natural Science Foundation of Gansu Province (23JRRA922); National Natural Science Foundation of China (52265049); Industrial Support Program for Colleges and Universities in Gansu Province (2022CYZC-26); Key Research and Development Plan Project of Gansu Province (23YFGA0054)
Corresponding author: Jia Zhi, Ph. D., Professor, School of Materials Science and Engineering, Lanzhou University of Technology, Lanzhou 730050, P. R. China, E-mail: jiazhi@lut.edu.cn

grains are elongated along the rolling direction after deformation, which inevitably leads to the preferred orientation of grains. Wang et al[18] studied the evolution of microstructure and texture of GH3536 superalloy under different cold rolling reductions. It was found that the textures were mainly S, Copper, Goss, and Brass types. Yu et al[19] found that due to the existence of hot-rolled texture, ZJ400 strip steel showed anisotropy in mechanical properties, which reduced its tensile strength and elongation. Basal texture is formed in the AZ31 magnesium alloy after rolling at room temperature, which leads to inhomogeneous deformation[20]. Therefore, the grain refinement by rolling technique will inevitably affect the properties and texture of the materials.

In order to better understand the effect of rolling deformation on the microstructure and mechanical properties of Inconel 617 alloy, this research conducted rolling process at room temperature to refine the grain size. The plastic deformation of Inconel 617 alloy was realized. The grain refinement and texture evolution of the samples with different deformation degrees were analyzed by electron backscatter diffraction (EBSD) and X-ray diffraction (XRD). In addition, the variation mechanism of microhardness and tensile properties was discussed. This research provided guidance for the investigation of the microtextures and mechanical properties of Inconel 617 alloy during rolling deformation.

1 Experiment

The chemical composition of the commercial Inconel 617 alloy was Cr=20.80wt%, Mo=9.12wt%, Al=1.28wt%, Co=13.10wt%, Fe=0.80wt%, C=0.07wt%, Si=0.11wt%, Ti=0.22wt%, and balanced Ni. The initial Inconel 617 alloy was solution treated at 1150 °C for 60 min. Solid solution strengthening elements (Cr, Co, Mo) accounted for 43.20wt% of the Inconel 617 alloy. The square sample of 60 mm×30 mm×10 mm was machined via wire electrical discharge machining. Then, multi-pass rolling was conducted, the deformation degree of each pass was 10%, and finally the cold rolled samples with total deformation degrees of 20%, 50%, and 70% were obtained. Besides, the original alloy (without cold rolling deformation) was also investigated as reference group.

The room temperature microhardness of the Inconel 617 alloy was measured using a microhardness tester. The microhardness test load was 0.1 kg, the loading time was 15 s, and at least 15 points of each sample were tested to obtain the average value. The dog-bone shaped samples with size of 25 mm×6 mm×1.5 mm were prepared by slow wire cutting and mechanical polishing. The tensile properties of the Inconel 617 alloy were tested by a uniaxial tensile testing machine, and the tensile rate was 1 mm/min. To ensure the repeatability of the experimental results, at least three tensile tests were performed under each set of experiment parameters.

The crystallographic structure of the Inconel 617 alloy with different deformation degrees was analyzed by XRD. The diffraction source was Cu target material (λ=0.154 06 nm). The voltage, current, step length, and scanning range were set as 40 kV, 150 mA, 5°/min, and $10° \leqslant 2\theta \leqslant 90°$, respectively. Microstructure and grain size were observed by EBSD. EBSD samples of 10 mm×10 mm×5 mm were firstly cut, then polished by mechanical grinding, and finally electropolished in the solution containing 90 mL C_2H_5OH and 10 mL $HClO_4$. EBSD data were processed using Channel 5 software.

2 Results and Discussion

2.1 Microstructure evolution

Fig. 1 shows the grain boundary distribution maps of Inconel 617 alloy under different deformation degrees. RD indicates the rolling direction and ND indicates the normal direction. The black lines represent the high-angle grain boundaries (θ>15°) and the green lines represent the low-angle grain boundaries ($2° < \theta \leqslant 15°$). The microstructure of original Inconel 617 alloy is composed of nearly equiaxed grains with an average grain size of 47.36 μm, and there are sparse low-angle grain boundaries in the intact grains (Fig.1a). Compared with the original microstructure, the deformed grains are significantly refined. After 20% deformation, the grains are elongated along RD, and a large number of low-angle grain boundaries are gathered around the high-angle grain boundaries (Fig.1b) with the average grain size of 15.98 μm. The grains of Inconel 617 alloy after 50% deformation are obviously elongated, and the low-angle grain boundaries exist uniformly in the grains (Fig. 1c). After 70% rolling deformation, Inconel 617 alloy exhibits elongated grains along RD, which is similar to the lamellar structure. Fine equiaxed grains appear in the elongated grains with the average grain size of 2.85 μm (Fig. 1d). This obvious grain refinement is caused by the increase in dislocation density in Inconel 617 alloy during the cold rolling process, which destroys the original grain boundaries. In order to release the deformation energy, dislocations are reorganized and gradually evolve into small grains. In other words, grain fragmentation occurs. The larger the deformation degree, the higher the dislocation density, the larger the strain, and the more obvious the grain refinement.

Fig. 2 shows the inverse pole figures of Inconel 617 alloy with different deformation degrees, and different colors represent different orientations. It can be observed from Fig.2a that the original grains are mainly (111) and (001) planes. The orientation of each individual grain is basically the same, indicating that the strain is small. When the deformation degree is 20%, the orientations of individual grains are changed, which is caused by the accumulation of dislocations. When the deformation degree is 50%, two kinds of orientation regions appear in some deformed grains. However, there are no high-angle grain boundaries between the regions, indicating that the orientation gradient within the grains is very high at this time, and it is prone to fragmentation to form small grains. When the deformation degree is 70%, the deformed grains are gradually transformed into (111) planes, and the refined grains are (101) planes. This result indicates that with the increase in deformation degree, the accumulation

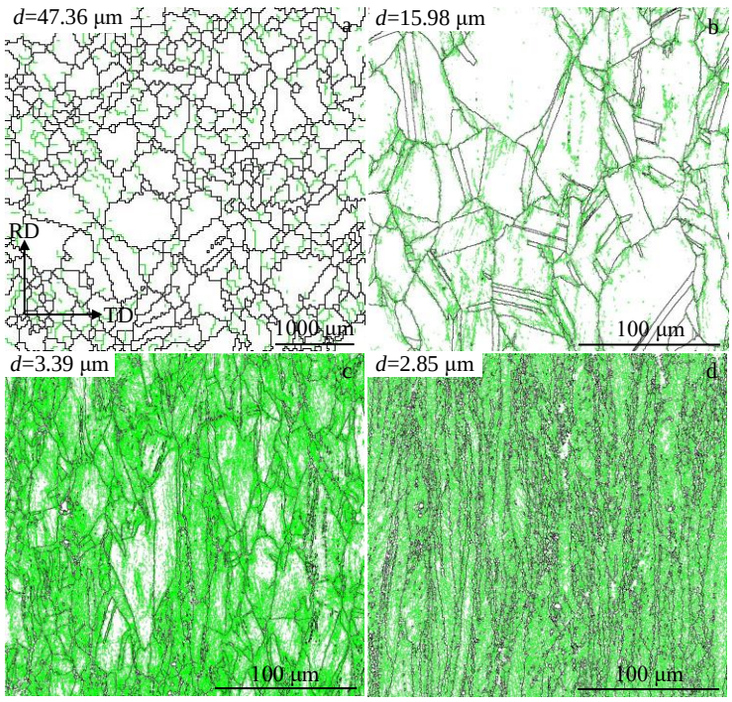

Fig.1 Grain boundary distribution maps of Inconel 617 alloy with different deformation degrees: (a) original, (b) 20%, (c) 50%, and (d) 70%

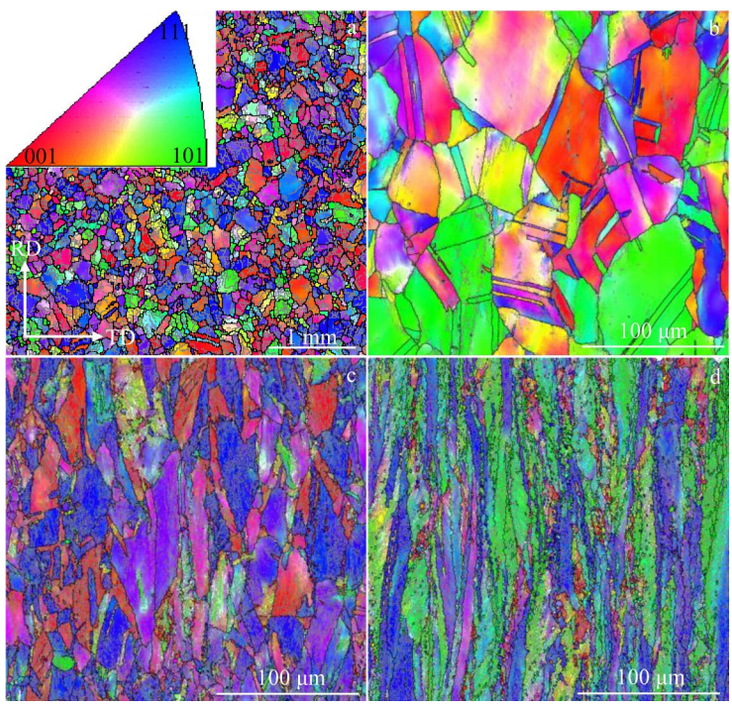

Fig.2 Inverse pole figures of Inconel 617 alloy with different deformation degrees: (a) original, (b) 20%, (c) 50%, and (d) 70%

of dislocations within the deformed grains leads to strain gradient to destroy the original grains, thereby refining the grains. In addition, with the increase in deformation degree, the grain refinement mainly results in the transformation from (111) plane to (110) plane.

2.2 XRD analysis

Fig. 3 shows XRD patterns of Inconel 617 alloy with different deformation degrees. Obviously, no new peak appears in Inconel 617 alloy after cold rolling, which indicates that no phase transformation occurs. The full width at half maximum is increased with the increase in deformation degree, illustrating the reduction in grain size. For polycrystalline materials, the number of grains arranged in the same direction plays a decisive role in the intensity of XRD diffraction peaks of the corresponding crystal planes. With the increase in deformation degree, the preferred orientation of

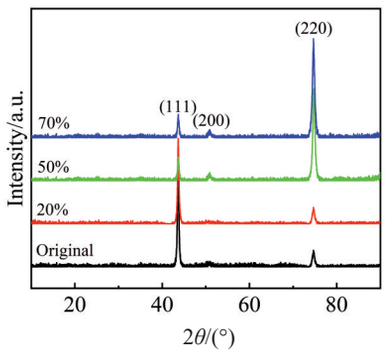

Fig.3 XRD patterns of Inconel 617 alloy with different deformation degrees

Table 1 Main diffraction peak intensities and texture coefficients of Inconel 617 alloy with different deformation degrees

Deformation degree	Intensity/cps			$TC_{(hkl)}$/%		
	(111)	(200)	(220)	(111)	(200)	(220)
Original	5360	246	765	84.13	3.86	12.01
20%	3972	155	1093	76.09	2.97	20.94
50%	896	320	4290	16.27	5.81	77.92
70%	815	380	4606	14.05	6.55	79.40

the Inconel 617 alloy becomes more obvious. This means that the dominate plane of the Inconel 617 alloy changes from the (111) plane to the (220) plane during the grain refinement of cold rolling deformation. This result is consistent with the analysis results of Fig.2.

Based on XRD patterns, the preferred orientation of the crystal planes can be estimated according to the diffraction peak intensity through the following formula[21]:

$$TC_{(hkl)} = \frac{I_{i(hkl)}}{I_{0(hkl)}}\left\{\sum_{i=1}^{N}\frac{I_{i(hkl)}}{I_{0(hkl)}}\right\}^{-1} = \frac{I_{(hkl)}}{\sum_{i=1}^{n} I_{(hkl)}} \quad (1)$$

where $TC_{(hkl)}$ is the relative texture coefficient, $I_{(hkl)}$ is the diffraction peak intensity of the (hkl) crystal plane, $I_{0(hkl)}$ is the diffraction peak intensity of the (hkl) crystal plane in the standard PDF card, and N is the number of total planes. The texture coefficients of the crystal planes corresponding to the main diffraction peaks are calculated, as listed in Table 1. It can be found that the value of $TC_{(220)}$ is increased with the increase in cold rolling deformation degree. Therefore, the change in diffraction peak intensity of Inconel 617 alloy is caused by the preferred orientation during cold rolling deformation.

2.3 Texture evolution

The orientation distribution function (ODF) cannot only determine the texture type but also quantitatively analyze the intensity of texture. Fig. 4 shows the positions of special orientation fibers and standard texture distributions of a face-centered cubic metal in the Euler space. The special orientation fibers include α-fiber, β-fiber, γ-fiber, and τ-fiber. Fig.5 shows ODF maps of the Inconel 617 alloy at φ_2=0°, 45°, and 65° in Euler space with different deformation degrees. It can be observed from Fig.5a that the main texture types of the original materials are Rotated Cube, Cube, and Rotated Copper textures, and the maximum texture intensity is 3.13. When the deformation degree is 20%, the main texture types are Brass, P, Rotated Copper, Goss, and S textures, and the maximum texture intensity is 7.98 (Fig. 5b). When the deformation degree is 50%, the P, Brass, and Goss textures almost disappear, the Copper texture is significantly enhanced, and the Shear1 {111} <110> is formed (Fig. 5c). When the deformation degree is increased to 70%, the main texture types are Goss, Brass, P, Rotated Copper, and Shear2 {111}<112> textures, and the maximum texture intensity is 13 (Fig. 5d). Therefore, the Shear1 {111} <110> texture is transformed into Shear2 {111} <112> texture, when the deformation degree increases from 50% to 70%. The main microtexture of the rolled samples is Goss {011} <001>, Rotated Goss {110} <110>, Brass {011} <211>, and P {011} <112> textures. With the increase in deformation degree, the texture intensity is also increased. This is because the stress direction of the sample does not change during the unidirectional rolling process, and the grain orientation tends to be consistent, resulting in the increased texture strength[22–23]. However, it is worth noting that the transformation of texture types may be related to the grain refinement process.

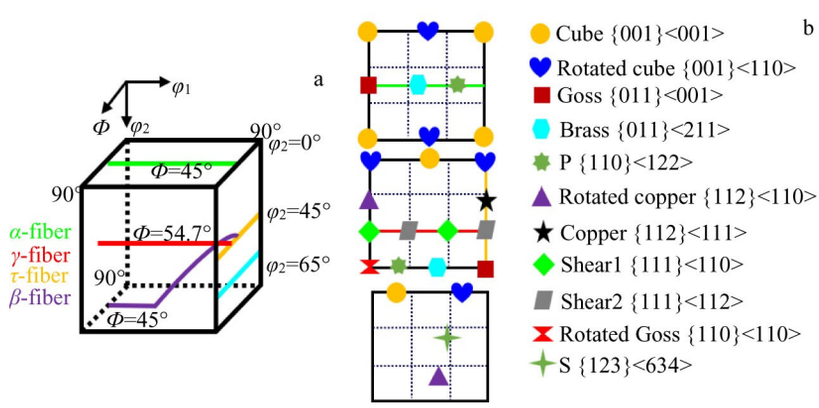

Fig.4 Positions of special orientation fibers (a) and standard textures (b) in Euler space

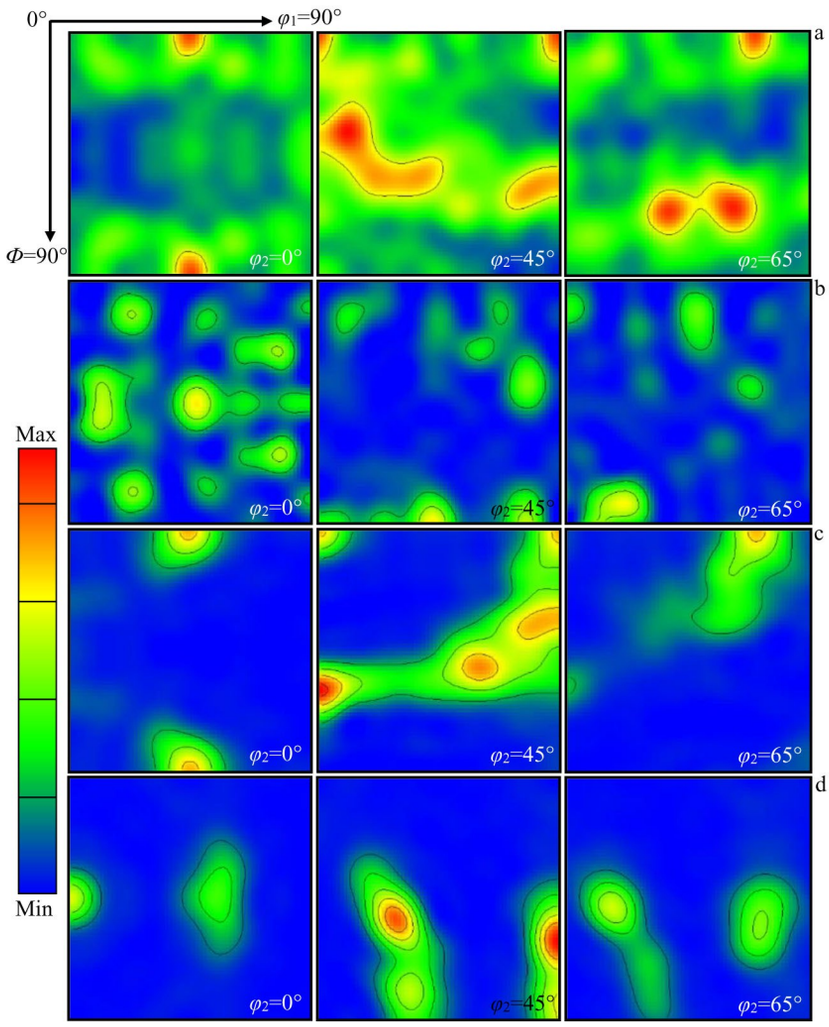

Fig.5 ODF maps in Euler space of Inconel 617 alloy with different deformation degrees: (a) original, (b) 20%, (c) 50%, and (d) 70%

Fig. 6 shows the quantitative analysis results of the orientation intensity, namely ODF value, of the microtextures during the cold rolling process of Inconel 617 alloy. The microtextures on α-fiber, γ-fiber, and τ-fiber in Euler space were selected for analysis. It can be found that the texture types on the α-fiber are mainly Brass and Rotated Goss (Fig. 6a). When the deformation degree is 20%, the micro-texture intensity on the α-fiber is enhanced, and the main microtextures are Brass and Rotated Goss textures. But the sample after 50% deformation has almost no microtexture on the α-fiber. After 70% deformation, the microtextures of the sample are significantly enhanced, and the main microtexture is Rotated Goss texture. There are Shear1 and Shear2 microtextures on the γ-fiber, as shown in Fig. 6b. It can be found that the shear texture intensity is increased with the increase in deformation degree. On the τ-fiber, the texture of the sample after 20% deformation does not appear, and the texture of the sample after 50% deformation is mainly Copper texture. With the increase in deformation degree, the Copper texture is gradually changed to Goss texture. Sekine et al[24] found that in the cold rolling process of metals with low stacking fault energy, when the deformation degree is large, the grains with Copper orientation tend to be twinned, i.e., the grains are transformed from {112} <111> to {554} <225>. Fig. 6d shows the main microtextures of Inconel 617 alloy with different deformation degrees. It can be found that with the increase in cold rolling deformation degree, the proportions of deformation microtextures (S, Copper, Brass) and Goss texture are increased, and the proportion of Cube texture is decreased. When the cold rolling deformation degree is 70%, the proportion of deformation microtextures reaches 79.36%.

2.4 Microhardness

The microhardness of the metal materials reflects the strain hardening ability and deformation resistance of the local area near the indentation[25]. In other words, the higher the microhardness, the better the plastic deformation resistance. Fig. 7 shows the average microhardness of Inconel 617 alloy with different deformation degrees. With the increase in deformation degree, the microhardness is also increased, which is conducive to the plastic deformation resistance. It is well known that the plastic deformation resistance is related to the density and free energy of dislocations. Roll deformation induces high strain and high dislocation density into Inconel

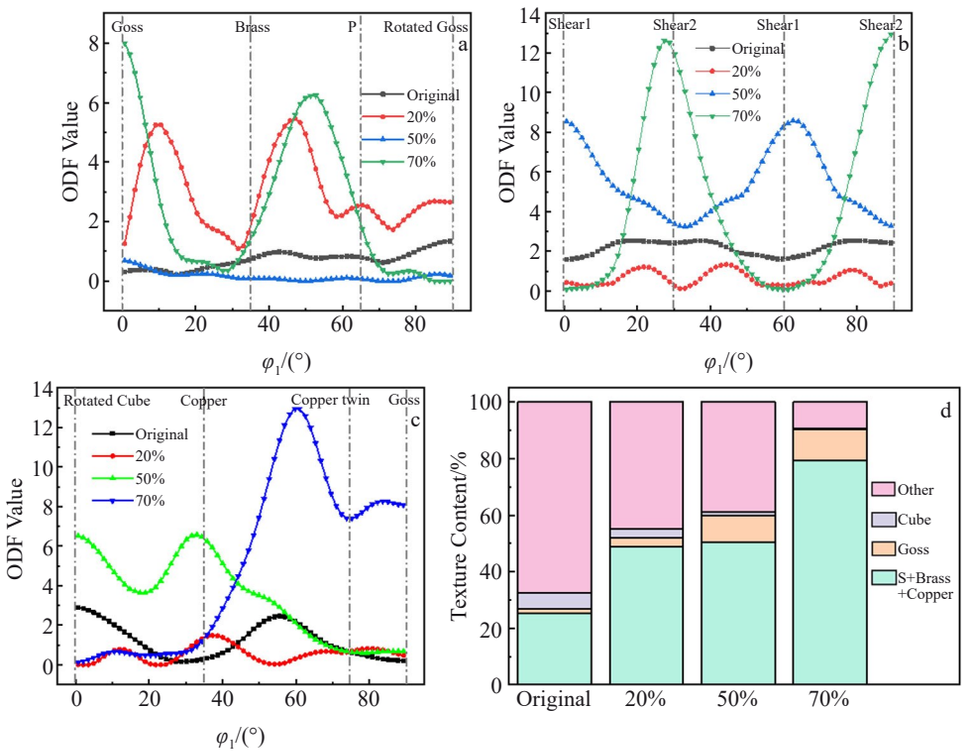

Fig.6 Microtexture intensities on special orientation fibers in Euler space (a–c) and texture contents (d) of Inconel 617 alloy with different deformation degrees: (a) α-fiber, (b) γ-fiber, and (c) τ-fiber

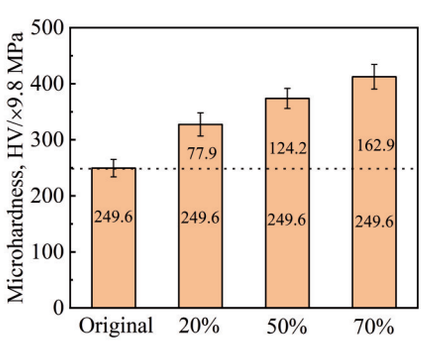

Fig.7 Microhardness of Inconel 617 alloy with different deformation degrees

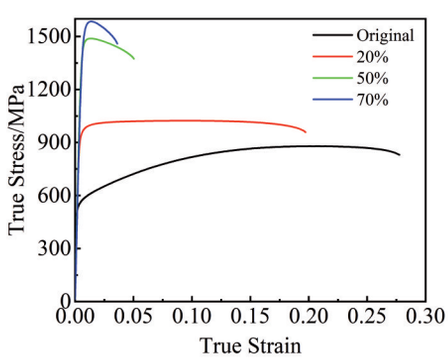

Fig.8 True stress-true strain curves of Inconel 617 alloy with different deformation degrees

617 alloy, which contributes to the hindrance of dislocation movement, therefore improving the plastic deformation resistance. In addition, the fine grains can effectively impede the dislocation movement, thus enhancing the microhardness. When the deformation degree is 70%, the microhardness is 4037.6 MPa, which is higher than that of the original sample by 65%.

2.5 Tensile properties

Fig. 8 shows the true stress-true strain curves of Inconel 617 alloy under different deformation degrees. It can be seen that the strength of Inconel 617 alloy increases and the elongation decreases after deformation. The change in strength and elongation is attributed to the grain refinement and the increased dislocation density after cold rolling. The strength and elongation of Inconel 617 alloys under different deformation degrees are shown in Table 2. It can be found that after 20% deformation, the yield strength of Inconel 617 alloy increases by 61.2% and elongation decreases by 29.3%, compared with those of the original sample. With the further increase in deformation degree, the yield strength is increased significantly, but the elongation is less than 5% (after 70% deformation). After 20% deformation, the cold rolled sample has the significantly refined grains with average grain size of 15.98 μm. However, the low-angle grain boundaries and orientation gradients are relatively small at this time. Thus, the synergy effect of strength enhancement and slight elongation reduction is achieved. However, after 50% and 70% deformation, the increase in dislocations and strains leads to the decrease in elongation even with more refined grains. Comprehensively, the yield strength and

Table 2 Mechanical properties of Inconel 617 alloy with different deformation degrees

Deformation degree	Yield strength, $\sigma_{0.2}$/MPa	Ultimate tensile strength, σ_b/MPa	Elongation, δ	Work hardening exponent, n
Original	479.18±18.4	879.45±26.1	0.2776±0.05	0.2196
20%	772.48±23.7	1023.37±43.4	0.1962±0.03	0.1357
50%	1326.9±40.2	1488.67±46.8	0.0503±0.02	0.0576
70%	1495.8±35.3	1584.67±45.6	0.0361±0.02	0.0257

elongation of Inconel 617 alloy after 20% deformation are 772.48 MPa and 0.1962, respectively, presenting good synergy effect.

The true stress-true strain curve of metallic materials follows the Hollomon equation[26]:

$$\sigma = K\varepsilon^n \quad (2)$$

where K is the strength coefficient and n is the work hardening exponent. Take logarithm of both sides of Eq.(2):

$$\ln\sigma = \ln K + n\ln\varepsilon \quad (3)$$

Fig. 9 shows the lnσ-lnε curves of Inconel 617 alloy with different deformation degrees. The plastic deformation stage in the lnσ-lnε curve is linearly fitted by $y=a+bx$, and the slope of the fitted line is the work hardening exponent n, namely the strain value of fracture occurrence in the tensile process. The calculated mechanical properties of the Inconel 617 alloy with different deformation degrees are shown in Table 2. Generally, the strength and elongation of the Inconel 617 alloy can be well coordinated when the deformation degree is 20%.

The tensile fracture morphologies of Inconel 617 alloy with different deformation degrees are shown in Fig. 10. Many dimples with different sizes can be observed in the fracture morphologies of the original sample and the sample after 20% deformation. Dimples are micropores formed by

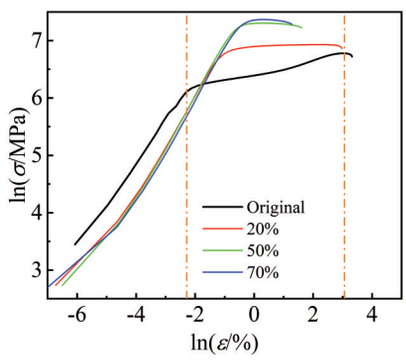

Fig.9 lnσ-lnε curves of Inconel 617 alloy with different deformation degrees

tearing when the materials with high elongation undergo plastic deformation. This result indicates that the original sample is mainly dominated by ductile fracture. With the increase in tensile force, the micropores are gradually increased, become larger, and finally pass through the grains, resulting in the typical transgranular fracture. According to the fracture morphologies of the samples after 50% and 70% deformation, the river-like patterns composed of dense cleavage steps can be observed, which is a typical brittle fracture feature.

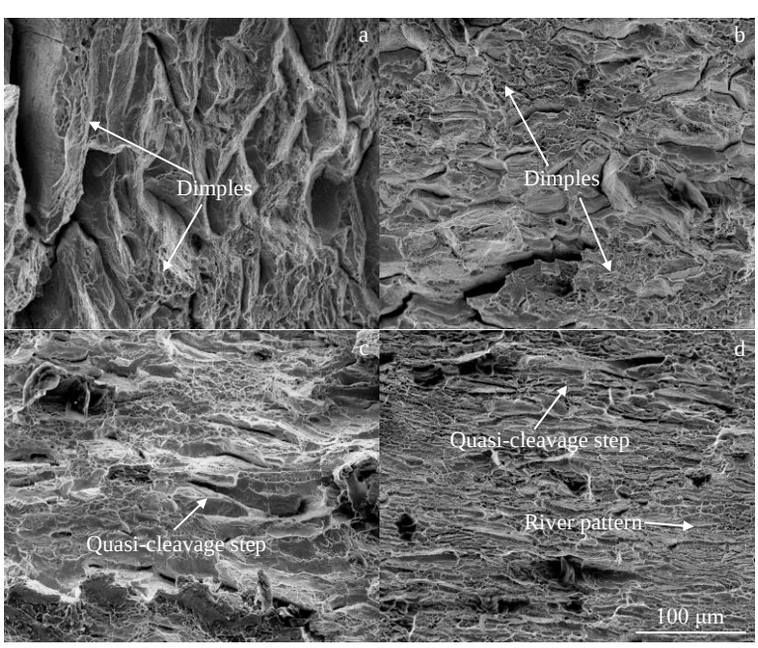

Fig.10 Tensile fracture morphologies of Inconel 617 alloy with different deformation degrees: (a) original, (b) 20%, (c) 50%, and (d) 70%

3 Conclusions

1) After rolling deformation, the proportion of low-angle grain boundaries of Inconel 617 alloy increases, and the strain gradient increases. Thus, the original grains fragment, and fine grains are formed.

2) The original Inconel 617 alloy has free orientation, and the proportion of deformation microtextures (S, Brass, Copper) increases after cold rolling. After 70% deformation, the proportion of deformation microtexture is 79.36%.

3) When the rolling deformation degree is more than 50%, Inconel 617 alloy has a strong shear texture, and with the increase in rolling deformation, the shear texture changes from Shear1 {111}<110> to Shear2 {111}<112>.

4) With the increase in deformation degree, the microhardness and strength of Inconel 617 alloy are increased, whereas the elongation is decreased. When the deformation degree is 20%, the strength and elongation of Inconel 617 alloy are well coordinated, presenting good synergy effect.

References

1 Hu Honglei, Zhao Mingjiu, Rong Lijian. *Rare Metal Materials and Engineering*[J], 2020, 49(1): 131 (in Chinese)
2 Salari S, Rahman M S, Beheshti A *et al*. *Mechanics Research Communications*[J], 2022, 121: 103875
3 Ji J J, Wang Y J, Yu L D *et al*. *Rare Metal Materials and Engineering*[J], 2023, 52(4): 1244
4 Bai Yaguan, Nie Yihong, Kou Jinfeng *et al*. *Rare Metal Materials and Engineering*[J], 2022, 51(1): 327 (in Chinese)
5 Hosseini H S, Shamanian M, Kermanpur A. *Materials Characterization*[J], 2011, 62(4): 425
6 Visweswara R C, Santhi S N C, Sastry G V S *et al*. *Materials Science and Engineering A*[J], 2021, 800: 140317
7 Jiang Mengling, Chen Yanhui, Kong Bin *et al*. *Titanium Industry Progress*[J], 2023, 40(4): 35 (in Chinese)
8 Jing Xiaoyan, Yuan Yi, Yu Fang *et al*. *Rare Metal Materials and Engineering*[J], 2009, 38(7): 1154 (in Chinese)
9 Anand M, Das A K. *Journal of Alloys and Compounds*[J], 2022, 929: 166949
10 Chen Jiayu, Yu Qiuying, Dong Jianxin *et al*. *Rare Metal Materials and Engineering*[J], 2017, 46(10): 2929 (in Chinese)
11 Zhang H B, Zhao W, Huang D *et al*. *Journal of Manufacturing Processes*[J], 2023, 108: 280
12 Li W, Cao Y, Huang G J *et al*. *Journal of Materials Research and Technology*[J], 2024, 28: 730
13 Xin Z, Jiang Y B, Wu Z X *et al*. *Materials Characterization*[J], 2023, 207: 113557
14 Wang X M, Ding Y T, Gao Y B *et al*. *Materials Science and Engineering A*[J], 2021, 823: 141739
15 Polkowska A, Lech S, Polkowski W. *Materials Science and Engineering A*[J], 2020, 787: 139478
16 Liu T, Zheng Q, Cheng X N *et al*. *Materials Science and Engineering A*[J], 2022, 850: 143549
17 Luo J T, Chu R H, Yu W L *et al*. *Journal of Alloys and Compounds*[J], 2019, 799: 302
18 Wang Y Q, Yuan C, Wei J X *et al*. *Journal of Materials Research and Technology*[J], 2023, 24: 2743
19 Yu Hao, Kang Yonglin, Liu Delu *et al*. *Chinese Journal of Engineering*[J], 2001, 23(6): 526 (in Chinese)
20 Tang Weiqin, Zhang Shaorui, Fan Xiaohui *et al*. *The Chinese Journal of Nonferrous Metals*[J], 2010, 20(3): 371 (in Chinese)
21 Wang Y, Tang W, Zhang L. *Journal of Materials Science and Technology*[J], 2015, 31(2): 175
22 Milner J L, Abu-Farha F, Kurfess T *et al*. *Materials Science and Engineering A*[J], 2014, 619: 12
23 Godoi R P, Zanquetta B D, Rubert J B *et al*. *Materials Science Forum*[J], 2021, 1016: 715
24 Sekine K, Wang J. *Materials Transactions, JIM*[J], 1999, 40(1): 1
25 Guo Y, Wang S R, Liu W T *et al*. *Tribology International*[J], 2020, 144: 106138
26 Li Y S, Zhang Y, Tao N R *et al*. *Acta Materialia*[J], 2009, 57(3): 761

晶粒细化对Inconel 617合金微观织构和力学性能的影响

姬金金[1,2,3]，贾　智[1,2]，杨佩瑶[1,2]，汪彦江[1,2]，寇生中[1,2]

(1. 兰州理工大学 材料科学与工程学院，甘肃 兰州 730050)

(2. 兰州理工大学 省部共建有色金属先进加工与再利用国家重点实验室，甘肃 兰州 730050)

(3. 兰州工业学院 材料工程学院，甘肃 兰州 730050)

摘　要：研究了室温轧制后不同变形量（20%、50%、70%）下的Inconel 617合金微观组织特征和力学性能变化。采用电子背散射衍射、X射线衍射分析了轧制过程中Inconel 617合金的晶粒细化机制和主要织构种类，并且对不同变形量下的Inconel 617合金的显微硬度和拉伸性能进行了测试。结果表明：在轧制变形过程中，Inconel 617合金晶粒发生细化，细化的机制是位错密度和应变梯度增大导致的原有晶粒破碎。轧制试样主要织构为高斯{011}<001>、旋转高斯{110}<110>、黄铜{011}<211>和P织构{011}<112>，并且随着变形程度的增大，剪切织构逐渐增强。轧制变形后，晶粒细化和位错强化共同提高了Inconel 617合金的强度，降低了塑性。综合来看，在20%的变形量时，Inconel 617合金的屈服强度和韧性分别为772.48 MPa和0.1962，具有较好的协同效果。

关键词：Inconel 617合金；晶粒细化；微观织构；硬度；拉伸性能

作者简介：姬金金，女，1988年生，博士，兰州理工大学材料科学与工程学院，甘肃 兰州 730050，E-mail：617599947@qq.com